

# Performance of Precise Point Positioning using Current Triple-frequency GPS Measurements in Australia

## ***Viet Duong***

School of Science, RMIT University, Australia  
Phone: +61 4 1340 1871 Email: [viet.duong@rmit.edu.au](mailto:viet.duong@rmit.edu.au)

## ***Ken Harima***

School of Science, RMIT University, Australia  
Phone: +61 3 9925 3775 Email: [ken.harima@rmit.edu.au](mailto:ken.harima@rmit.edu.au)

## ***Suelynn Choy***

School of Science, RMIT University, Australia  
Phone: +61 3 9925 2650 Email: [suelynn.choy@rmit.edu.au](mailto:suelynn.choy@rmit.edu.au)

## ***Chris Rizos***

School of Civil and Environmental Engineering, University of New South Wales, Australia  
Phone: +61 2 9385 4205 Fax: +61 2 9385 6139 Email: [c.rizos@unsw.edu.au](mailto:c.rizos@unsw.edu.au)

## **ABSTRACT**

GNSS Network Real-Time-Kinematic (NRTK) has become a common service for many precise positioning applications over the last two decades. However, NRTK cannot service or support user applications if they are outside the Continuously Operating Reference Stations (CORS) network coverage area, such as in the case of offshore surveying. In addition, NRTK requires a fairly dense network of CORS (typically station separation <80 km) to generate reliable corrections for centimetre-level positioning, and ground communication channels to disseminate the corrections to users. Precise Point Positioning (PPP) is a viable alternative for some GNSS applications as it does not have the onerous requirement of a dense network of CORS infrastructure. However the current major limitation of the PPP technique is the slow solution convergence time (tens of minutes for the solutions to converge to decimetre-level accuracy). This is not adequate to support many real-time positioning and navigation applications requiring high accuracy positioning. This paper describes the prospects, effectiveness as well as challenges in using triple-frequency GPS measurements in a PPP model. In particular, the paper describes research into assessing the performance of triple-frequency PPP. One week of triple-frequency GPS observations from eight CORS stations in Australia were processed in static mode. The estimated positions were then compared with the known coordinates. The results indicate that the use of triple-frequency GPS measurements improves the 3D positioning accuracies as well as shortens solution convergence times compared to dual-frequency PPP.

**KEYWORDS:** Precise Point Positioning (PPP); Multi-constellation PPP; Triple-frequency PPP; Rapid convergence times; Ambiguity resolution.

## 1. INTRODUCTION

Recently, the Global Navigation Satellite System (GNSS) has become a popular service for civilian society. In fact, this technology can be applied to many positioning, navigation and timing (PNT) applications. Besides, the system also can provide a wide range of accuracies for users' applications from several metres to centimetres. In terms of high accuracy positioning services required by the surveying and construction industries, and precision agriculture, relative positioning techniques such as Real-Time-Kinematic (RTK) or Network Real-Time-Kinematic (NRTK) have been the preferred and dominant approaches. In general, the RTK technique requires at least two receivers tracking the same satellites simultaneously to obtain high accuracy positions in real-time. Many systematic errors are cancelled out when forming combinations of observations between the base and rover receivers. Depending on the density of Continuously Operating Reference Stations (CORS) in a local area, types of measurements observed (DGPS: code measurement or RTK: code and carrier-phase measurements), the obtained positioning accuracy using the relative technique could vary from centimetre- to submetre-level. However, the relative GNSS technique has its limitations. First, it cannot support users' applications if they are outside the network coverage such as in the case of offshore surveying. Second, areas with low density of CORS stations, or poor telecommunication coverage could also be a challenge for NRTK. Lastly, the cost required to establish a dense nationwide CORS network may not be justifiable for many developing nations.

Precise Point Positioning (PPP) is emerging as a cost-effective technique, which can supplement the high accuracy NRTK technique. Unlike NRTK, PPP only requires one GNSS receiver for positioning and a fairly sparse network of CORS stations. PPP is not constrained by the baseline length between CORS stations in order to produce high accuracy positioning. As a result, there is a reduction in labour, equipment costs, computation burden as well as simplified operational logistics (Rizos *et al.* 2012). It uses a robust modelling of GNSS errors and precise information on satellite orbits, satellite clocks and signal biases to make accurate estimates of the user position (Kouba 2009; Zumberge *et al.* 1997).

Many errors could be eliminated or reduced by applying the relative GNSS techniques, but the errors exist in the PPP model and must be considered in GNSS data processing. Kouba (2009) and Rizos *et al.* (2012) listed the error sources that must be considered when using PPP, e.g., receiver and satellite antenna offsets, phase wind-up, site displacement effects, solid earth tides, rotational deformation due to polar motion (polar tides), ocean loading and earth rotation parameters. Therefore, the ambiguity terms (as required for centimetre-accurate solutions) of the un-differenced phase observations in a PPP model cannot be resolved easily.

To enhance the performance of PPP in terms of reducing the ambiguity convergence time and improving positioning accuracy, the integer ambiguity in the phase measurement needs to be resolved. Zumberge *et al.* (1997) was one of the first to propose the use of un-differenced ionosphere-free linear combination based on dual-frequency GPS measurements to achieve sub-centimetre-level positioning. They noted that phase ambiguity resolution is valuable for improving the solution convergence time. Many research publications have investigated methods to reduce the convergence time of both wide-lane (WL) and ionosphere narrow-lane

(NL) integer ambiguity resolution in PPP (Collins 2008; Collins & Bisnath 2011; Ge *et al.* 2008; Geng 2010; Geng *et al.* 2010a; Laurichesse *et al.* 2009). Three main PPP ambiguity resolution methods have been developed, which include the decoupled clock model (Collins 2008), the single-difference between-satellite model (Ge *et al.* 2008), and the integer phase clock model (Laurichesse *et al.* 2008). The relationship between these PPP ambiguity resolution methods, and also their equivalences has been explored and described by Geng *et al.* (2010b), Shi and Gao (2013), and Teunissen and Khodabandeh (2014). The performance of PPP WL and NL integer ambiguity resolution has been analysed in several publications, such as Geng *et al.* (2010a), Laurichesse *et al.* (2010), and Shi (2012). Nonetheless, it is suggested that tens of minutes are required for reliable NL integer ambiguity resolution.

The use of triple-frequency GNSS signals is expected to improve PPP WL and NL integer ambiguity resolution compared to the dual-frequency case. Next generation GNSS such as the modernised GPS, Galileo and BeiDou satellites are already transmitting a third signal for positioning, e.g., the 12 GPS Block IIF satellites transmitting a signal on the L5 frequency band (Security 2016). Laurichesse (2015), Li *et al.* (2013), Geng and Bock (2013) and El-Mowafy *et al.* (2016) have suggested that the use of triple-frequency GNSS observations in PPP could enhance the converge time and positioning accuracy when compared to dual-frequency PPP. Alternatively, a hybrid system of PPP and NRTK could deliver rapid convergence time, and subsequently improved positioning performance (Choy *et al.* 2016; Teunissen & Khodabandeh 2014).

The motivation for this research is to extend the work of Laurichesse (2012, 2015, 2016), Li *et al.* (2013), Geng and Bock (2013), and El-Mowafy *et al.* (2016), who have proposed innovative techniques to reduce the convergence time in triple-frequency PPP, particularly in PPP WL integer ambiguity resolution. These publications describe the performance of dual- and triple-frequency PPP and then compare the results between the two processing scenarios using both simulated and real observations. However, static processing of actual data in these publications is limited by the geographical location of the GNSS stations used (mainly conducted at one CORS station in Europe) and the observation period (only about one-hour maximum). This is due to the limited number of GPS Block IIF satellites in view at a particular station around the world. Hence, the aim of this research is to provide an insight into the current performance of triple-frequency GPS PPP in Australia. The research will use real observations collected from eight Australian CORS stations over a one week period. The triple-frequency PPP results will be compared with dual-frequency PPP for both float and fixed ambiguities. In this work, the proposed algorithms in Laurichesse (2015, 2016), Li *et al.* (2013), Geng and Bock (2013) are implemented using a sequential Least Squares adjustment within a Matlab-based GPS PPP data processing software. The software was developed at RMIT University along with a modified version of the open source RTKLIB software (Takasu 2016).

In the next section, the mathematical model is described to highlight the differences between dual- and triple-frequency PPP. Then, Section 3 “Data Collections and Processing Strategy” describes the data used in the research and the processing methodology. Section 4 “Dual- and Triple-Frequency PPP Results” describes the performance of dual- and triple-frequency PPP, including positioning convergence time and the resultant ambiguity fixing rate. Some concluding remarks are given in the final section.

## 2. PPP MATHEMATICAL MODEL

In this paper, the mathematical model for dual- and triple-frequency PPP will be summarised using the single-difference between-satellite model, as it cancels out the receiver's clock error, phase and code biases.

### 2.1 Single-difference between-satellite model

The general formulas of un-differenced code and phase observations on  $i^{\text{th}}$  frequency (e.g.  $i = 1, 2$  and  $5$  for the GPS system) from receiver ( $r$ ) to satellite ( $s$ ) are denoted as (Geng & Bock 2013; Hofmann *et al.* 2008; Li *et al.* 2013):

$$L_{ir}^s = \rho_r^s + c(t_r - t^s) - \frac{f_1^2}{f_i^2} I_r^s + T_r^s + \lambda_i (B_{ir} - B_i^s) + \lambda_i N_{ir}^s + \mathcal{E}_{ir}^s \quad (1)$$

$$P_{ir}^s = \rho_r^s + c(t_r - t^s) + \frac{f_1^2}{f_i^2} I_r^s + T_r^s + (b_{ir} - b_i^s) + \nu_{ir}^s \quad (2)$$

where:

$L_{ir}^s$	is the raw phase measurement on the $i^{\text{th}}$ frequency (m)
$P_{ir}^s$	is the raw code measurement on the $i^{\text{th}}$ frequency (m)
$\rho_r^s$	is the geometric distance as a function of receiver and satellite coordinates (m)
$c$	is the speed of light in vacuum (m/s)
$\lambda_i$	is the wavelength of carrier phase on $i^{\text{th}}$ frequency (m)
$f_i$	is the $i^{\text{th}}$ frequency (MHz)
$I_r^s$	is the first order ionospheric delay (m)
$T_r^s$	is the tropospheric delay (m)
$b_{ir}, b^s$	is the code observable-dependent receiver and satellite bias (m)
$\lambda_i B_{ir}, \lambda_i B^s$	is the phase observable-dependent receiver and satellite bias (m)
$N_{ir}^s$	is the integer ambiguity on $i^{\text{th}}$ frequency (m)
$\nu_{ir}^s, \mathcal{E}_{ir}^s$	is unmodelled errors such as multipath effects and noise (m)

The single-difference for code and phase measurement ( $i^{\text{th}}$  frequency) between satellites (e.g.  $b$  and  $s$ ) is determined by:

$$P_{ir}^{bs} = \rho_r^{bs} + ct^{bs} + \frac{f_1^2}{f_i^2} I_r^{bs} + T_r^{bs} + b_i^{bs} + \nu_{ir}^{bs} \quad (3)$$

$$L_{ir}^{bs} = \rho_r^{bs} + ct^{bs} - \frac{f_1^2}{f_i^2} I_r^{bs} + T_r^{bs} + \lambda_i B_i^{bs} + \lambda_i N_{ir}^{bs} + \mathcal{E}_{ir}^{bs} \quad (4)$$

The receiver clock errors as well as the receiver phase and code biases are excluded by using (3) and (4). It also should be noted that PPP-related errors such as relativistic (Sagnac effect and earth rotation correction), phase wind-up along with receiver and satellite phase centre variations has been corrected in the geometric range and phase measurements, and not included in the mathematical model.

The satellite corrections, including clocks, orbits, code biases and phase biases (e.g. L1, L2

and L5), could be eliminated by using State Space Representation (SSR) products provided by the CLK93 (CNES 2016) real-time stream, and/or final products from the International GNSS Service (IGS) (IGS 2016).

## 2.2 Ambiguity Resolution in PPP

If a dual-frequency or triple-frequency GPS receiver is used, the ionosphere delay can be removed when forming linear combinations between these frequencies for both WL and NL integer ambiguities.

The integer ambiguity resolution in PPP is divided in two steps for dual-frequency measurements, and three steps for triple-frequency measurements.

### Dual-frequency PPP Ambiguity Resolution:

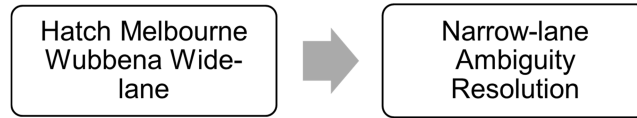


**Figure 1.** Flow chart for dual-frequency PPP data processing

#### Step 1: Hatch Melbourne Wubben wide-lane (MWWL) ambiguity resolution (L1&L2)

$$L_{mwr}^{bs} = \frac{f_1 L_{1r}^{bs} - f_2 L_{2r}^{bs}}{f_1 - f_2} - \frac{f_1 P_{1r}^{bs} + f_2 P_{2r}^{bs}}{f_1 + f_2} = \lambda_w N_w^{bs} + \phi_w^{bs} + \epsilon_w^{bs} \quad (5)$$

where  $\phi_w^{bs} = \frac{c}{f_1 - f_2} B_{12}^{bs} - \frac{f_1 b_1^{bs}}{f_1 + f_2} - \frac{f_2 b_2^{bs}}{f_1 + f_2}$  is the MWWL satellite biases including the uncalibrated phase delay (UPD) and the pseudorange code bias, with  $B_{12}^{bs} = B_1^{bs} - B_2^{bs}$ ; the wide-lane wavelength is defined as  $\lambda_w = \frac{c}{f_1 - f_2} = 0.862m$  and the single-differenced ambiguity and the linear combination noise level are  $N_w^{bs} = N_{12r}^{bs} = N_{1r}^{bs} - N_{2r}^{bs}$  and  $\sigma_w \approx 0.713\sigma_p$  respectively.

#### Step 2: Narrow-lane ambiguity resolution (L1&L2)

Ionosphere-free NL model with the assistance of ionosphere-free pseudorange

$$\begin{cases} P_{nlr}^{bs} = \frac{f_1^2}{f_1^2 - f_2^2} P_{1r}^{bs} - \frac{f_2^2}{f_1^2 - f_2^2} P_{2r}^{bs} \\ L_{nlr}^{bs} = \frac{f_1^2}{f_1^2 - f_2^2} L_{1r}^{bs} - \frac{f_2^2}{f_1^2 - f_2^2} L_{2r}^{bs} \end{cases} \quad (6)$$

where  $L_{nlr}^{bs}$  can be further expressed in more detail:

$$L_{nlr}^{bs} - \frac{\lambda_2 f_2^2}{f_1^2 - f_2^2} N_w^{bs} = \rho_r^{bs} + ct^{bs} + T_r^{bs} + \frac{c}{f_1 + f_2} N_{1r}^{bs} + \frac{\lambda_1 f_1^2}{f_1^2 - f_2^2} B_1^{bs} - \frac{\lambda_2 f_2^2}{f_1^2 - f_2^2} B_2^{bs} \quad (7)$$

Similarly, the narrow-lane wavelength is  $\lambda_{nl} = \frac{c}{f_1 + f_2} = 0.107m$ , the single-differenced ambiguity on frequency L1 is written as  $N_{nl}^{bs} = N_{1r}^{bs}$ . The noise levels for code and phase ionosphere-free combinations are  $\sigma_{Pnl} \approx 2.978\sigma_P$  and  $\sigma_{Lnl} \approx 2.978\sigma_L$ .

### Triple-frequency PPP Ambiguity Resolution:

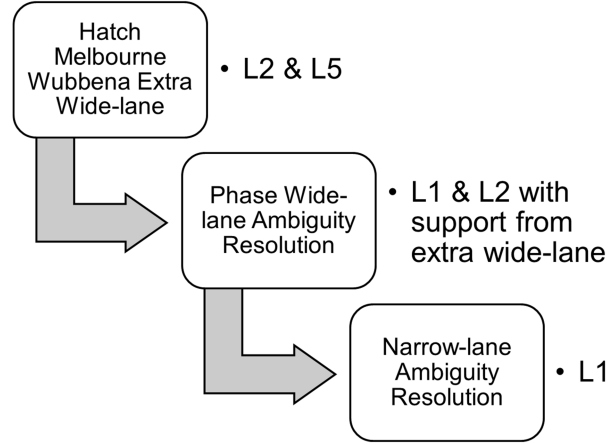


**Figure 2:** Flow chart for triple-frequency PPP

#### Step 1: Melbourne Wubben Extra-widelane (EWL) ambiguity resolution (L2&L5)

$$L_{emw}^{bs} = \frac{f_2 L_2^{bs} - f_5 L_5^{bs}}{f_2 - f_5} - \frac{f_2 P_2^{bs} + f_5 P_5^{bs}}{f_2 + f_5} = \lambda_{ew} N_{ew}^{bs} + \phi_{ew}^{bs} + \varepsilon_{ew}^{bs} \quad (8)$$

The variables on the right hand side of (8) are described in more detail:

$$\begin{aligned} \frac{f_2 L_2^{bs} - f_5 L_5^{bs}}{f_2 - f_5} - \frac{f_2 P_2^{bs} + f_5 P_5^{bs}}{f_2 + f_5} &= \overbrace{\frac{c}{f_2 - f_5} N_{25r}^{bs}}^{\lambda_{ew}} + \overbrace{\frac{c}{f_2 - f_5} B_{25}^{bs} - \frac{f_2 b_2^{bs}}{f_2 + f_5} + \frac{f_5 b_5^{bs}}{f_2 + f_5}}^{\phi_{ew}^{bs}} + \frac{c}{f_2 - f_5} \varepsilon_{25r}^{bs} \\ &- \frac{c}{f_2 + f_5} (v_2^{bs} + v_5^{bs}) \end{aligned}$$

where  $L_{ew}^{bs}$  and  $\varepsilon_{ew}^{bs}$  represent the EWL measurement and noise. The EWL integer ambiguities ( $N_{ew}^{bs} = N_{25r}^{bs} = N_{2r}^{bs} - N_{5r}^{bs}$ ) with a large wavelength, about  $\lambda_{ew} = \frac{c}{f_2 - f_5} = 5.861m$  for GPS, are expected to be fixed instantaneously. This linear combination has a noise level of about  $\sigma_{ew} \approx 0.727\sigma_P$ .

**Step 2:** A new model proposed by Geng and Bock (2013); Li *et al.* (2013) has been used for phase wide-lane ambiguity resolution in triple-frequency PPP.

When the conditions of geometry-based and ionosphere-free must be fulfilled and the constraint of extra-wide lane is fixed (known). The linear combination of three frequencies is written as:

$$LC_w^{bs} = xL_{1r}^{bs} + yL_{2r}^{bs} + zL_{5r}^{bs} \quad (9)$$

where the three conditions are:

$$\begin{cases} x + y + z = 1 \\ x + \frac{f_1^2}{f_2^2}y + \frac{f_1^2}{f_5^2}z = 0 \\ \lambda_1x + \lambda_2y + \lambda_3z = 0 \end{cases}$$

Equation (9) can be further expressed as:

$$LC_w^{bs} = \rho_r^{bs} + ct^{bs} + \lambda_{LC}(N_w^{bs} + B_{12}^{bs}) - \frac{f_5\lambda_{ew}}{(f_1 - f_5)}(N_{ew}^{bs} + B_{25}^{bs}) + \varepsilon_{wl}^{bs} \quad (10)$$

Although the noise level of the proposed WL in (10) is amplified to  $\sigma_{LC} \approx 110\sigma_L$ , the wide-lane wavelength for ambiguities using the resolved of the extra-widelane ambiguity is about

$$\lambda_{LC} = \frac{f_1}{f_1 - f_5} \times \frac{c}{f_1 - f_2} = 3.40m. \text{ This wavelength is much bigger than that in the standard}$$

dual-frequency case. As a result, (10) will facilitate rapid ambiguity resolution. In addition, Laurichesse (2015) states that the WL ambiguities can be fixed in about two minutes and also provide decimetre-level positioning accuracy, which is suitable for many applications that do not demand centimetre-level accuracy. Furthermore, Li *et al.* (2013) presents an optimal pseudorange linear combination that requires a minimal measurement noise, geometry-based and ionosphere-free (see (11) and three conditions).

$$PC^{bs} = xP_{1r}^{bs} + yP_{2r}^{bs} + zP_{5r}^{bs} \quad (11)$$

where the three conditions are:

$$\begin{cases} x + y + z = 1 \\ x + \frac{f_1^2}{f_2^2}y + \frac{f_1^2}{f_5^2}z = 0 \\ (x^2 + a^2y^2 + b^2z^2)\sigma_p^2 = \min \sigma_p^2 \end{cases}$$

Note:  $a$  and  $b$  are scaling factors for the triple-frequency measurement noises on L2 and L5.

PPP WL integer ambiguity resolution using (11) is expected to be possible more quickly than those of the Geng and Bock (2013) model because of the optimal triple-frequency pseudorange measurements ( $PC^{bs}, \sigma_{PC} \approx 2.54\sigma_p$  for the GPS system).

**Step 3:** In the narrow-lane step, (9) with the resolved EWL and WL integer ambiguities can be used to constraint (7) as:

$$\begin{cases} LC_w^{bs'} = LC_w^{bs} - \lambda_{LC}(N_w^{bs} + B_{12}^{bs}) + \frac{f_5\lambda_{ew}}{(f_1 - f_5)}(N_{ew}^{bs} + B_{25}^{bs}) = \rho_r^{bs} + ct^{bs} + \varepsilon_w^{bs} \\ L_{nlr}^{bs} = \frac{f_1^2}{f_1^2 - f_2^2}L_{1r}^{bs} - \frac{f_2^2}{f_1^2 - f_2^2}L_{2r}^{bs} \end{cases} \quad (12)$$

Instead of using the code combination as shown in (6), (12) uses the resolved EWL and WL

integer ambiguities as an additional phase measurement with noise amplified by  $\sigma_{LC} \approx 110\sigma_L$ . It is anticipated that the performance of triple-frequency PPP NL ambiguity resolution such as in (12) would give a better solution compared with dual-frequency PPP such as in (6). This is because a new form of code measurement established from a combination of three phase measurements ( $LC_w^{bs}, \sigma_{LC} \approx 110\sigma_L$ ) as shown in (12) has less noise than using a linear combination for code measurement ( $P_{nlr}^{bs}, \sigma_{Pnlr} \approx 2.98\sigma_p$ ) as shown in (6). For example, if carrier-phase precision  $\sigma_L$  is close to 2mm, which is common for most present high-grade GPS receivers, the precision of  $LC_w^{bs}$  is far better than  $P_{nlr}^{bs}$ .

If the variances of phase and pseudorange measurements are equal on three frequencies for GPS, and the variance of phase measurement are much smaller than that of the pseudorange

$$\sigma_{L1} = \sigma_{L2} = \sigma_{L5} = \sigma_L;$$

measurement. In other words,  $\sigma_{p1} = \sigma_{p2} = \sigma_{p5} = \sigma_p$ ;

$$\sigma_L \ll \sigma_p$$

It is also worth mentioning that the error sources such as phase wind-up or satellite hardware biases are well modelled and corrected beforehand, the benefits of triple-frequency compared with dual-frequency for integer ambiguity resolution are summarized briefly as table below:

Steps	Wavelengths (m)		Noise levels of combinations		Parameters		Possible advantages for using triple-frequency
	Dual	Triple	Dual	Triple	Dual	Triple	
<b>EWL</b>	Not applied	5.86	Not applied	$0.7\sigma_p$	Not applied	$N_{ew}^{bs}$	<i>Ambiguities Resolved instantaneously</i>
<b>WL</b>	0.86	3.40	$0.7\sigma_p$	$110\sigma_L$	$N_w^{bs}$	U+ T+ $N_w^{bs}$	<i>WL ambiguities can be fixed in about two minutes Providing decimetre-level positioning accuracy</i>
<b>NL</b>	0.107	0.108	$2.98\sigma_L$ $2.98\sigma_p$	$2.54\sigma_L$ $110\sigma_L$	U+ T+ $N_1^{bs}$	U+ T+ $N_1^{bs}$	<i>An optimal combination for phase measurements with a low noise level Using the support of WL and EWL to create a new form "code measurement"</i>

with: User positions (U); tropospheric delay (T); and ambiguity terms (N)

In addition, cycle slips can be detected and corrected more easily using triple-frequency GPS measurements as described in Zhao *et al.* (2015).

### 3. DATA COLLECTION AND PROCESSING STRATEGY

A total of eight GNSS CORS stations from the Australian Regional GNSS Network (ARGN) were selected. The geographical location of the selected eight CORS stations is shown in Figure 3. The ITRF2008 coordinates realised from the Geoscience Australia analysis report (Geoscience-Australia 2016) along with the station receiver and antenna information is provided in Table 1.



The ARGN stations were selected based on two criteria. Firstly, it tracks a maximum number of GPS Block IIF satellites in view for a minimum observation period of 60 minutes; and secondly, the distribution of these CORS stations should be located in remote areas whereby the density of nearby CORS stations is low and there is limited telecommunication coverage. This is to simulate an environment where a NRTK service is not available to users.

To evaluate triple-frequency PPP performance compared to that of dual-frequency PPP, seven consecutive days of GPS observations from 30 July to 5 August 2016 (DOY 212 to 218) were processed. Only GPS measurements were used in this research.

**Table 1.** ITRF2008 coordinates at epoch @ 20/07/2016 at the eight selected GNSS CORS stations along with their receiver and antenna types

Stations	X (m)	Y (m)	Z (m)	Receiver types	Antenna types
ALIC	-4052052.6000	4212836.0011	-2545104.7716	LEICA GR25	LEIAR25.R3 +NONE
CUT0	-2364337.4976	4870285.6231	-3360809.5982	TRIMBLE NETR9	TRM59800.00 +SCIS
KARR	-2713833.1163	5303935.1115	-2269513.9396	TRIMBLE NETR9	TRM59800.00 +NONE
KAT2	-4147369.3926	4581537.0445	-1573259.8129	TRIMBLE NETR9	TRM59800.00 +NONE
LILY	-4037356.4508	2600427.5511	-4183584.2753	TRIMBLE NETR9	TRM59800.00 +NONE
STR2	-4467075.1234	2683011.8537	-3667007.2122	TRIMBLE NETR9	TRM59800.00 +NONE
TITG	-4956026.6575	3841248.2875	-1164089.4420	SEPT POLARXS	JAVRINGANT_DM+SCIS
TOW2	-5054583.2892	3275504.1616	-2091538.6512	SEPT POLARXS	LEIAR25.R3 + NONE

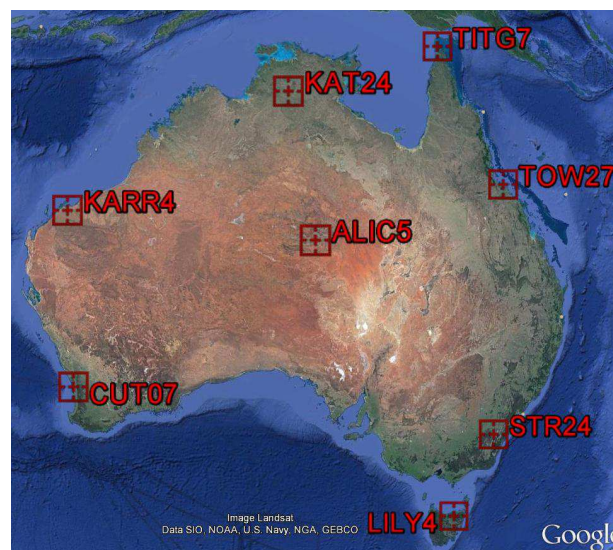


**Figure 3.** Eight selected CORS stations from the Australian Regional GNSS Network (Google Earth)

During the entire period of interest a maximum of four Block IIF satellites were often visible

simultaneously in Australia for an average period of 70 minutes. The total number of GPS satellites in view during this period is around seven to eight satellites. Figure 4 is an example showing the number of GPS Block IIF satellites in view at the ALIC station on DOY215 2016.

There were two 70 minute observation sessions per a day for each station based on the current GPS satellite orbit configuration. Thus, the total number of datasets available for this research is 112. The GPS measurements were recorded at one-second sampling interval.

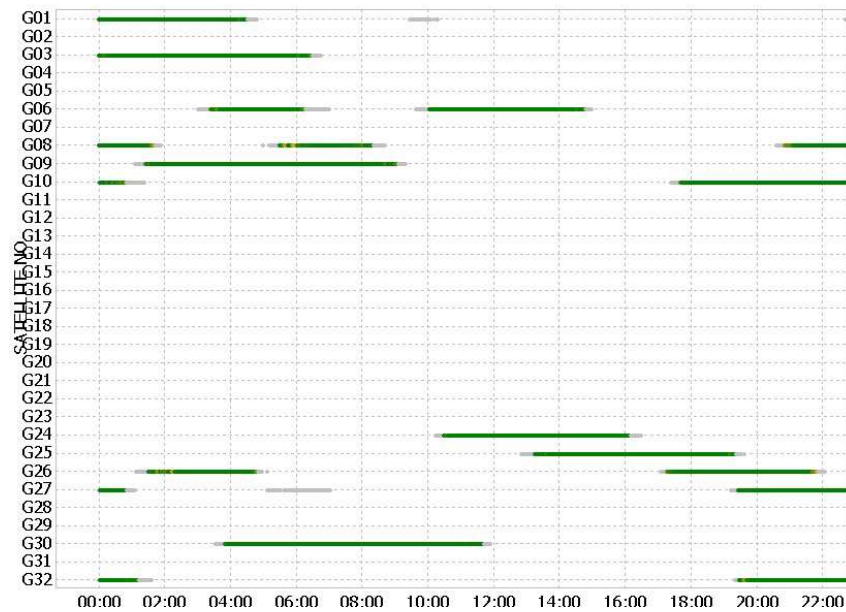


**Figure 4:** Visibility of the GPS Block IIF satellites transmitting L5 signal at the ALIC station on DOY 215 2016

A module of the RTKLIB software (Takasu 2016) was used to stream the GPS data from the eight selected CORS stations. Then a modified version of RTKLIB output the corrected GPS observables. Lastly, Matlab-based GPS PPP data processing software was developed to process the corrected observables using both dual- and triple-frequency data. The LAMBDA algorithm (Teunissen 1993) was used for resolving integer ambiguities. Particularly, the integer least-square method was used for resolving the PPP EWL, WL and NL ambiguities. Furthermore, the quality control of integer ambiguity resolution has been used the model-driven ratio test with fixed failure rate proposed by Verhagen and Teunissen (2013). A high threshold for the success rate with 99.99% was set for data processing, so the performance of dual- and triple- frequency PPP is reliably evaluated. The processing parameters used are listed in Table 2.

**Table 2.** Software parameters used in the modified RTKLIB to output the corrected GPS observables

Items	Models/Constraints
Station position	Static: PPP-fixed
Observations	- Ionosphere-free combination measurements - GPS: L1/L2/L5 - Elevation-dependent weighting strategy
Elevation Cut-off Angle	$10^0$
Sampling Rate	1s
Precise Satellite Orbit,	CLK93

Clock, Code & Phase biases	
Satellite PCO & PCV, and Receiver PCO & PCV	GPS: IGS antenna products (IGS08_1904.atx)
Phase wind-up	Corrected
Ionosphere	First-order effect removed by ionosphere-free combination
Troposphere model	Zenith hydrostatic delay is obtained by Saastamoinen model using a standard atmospheric model. Zenith wet delay and the gradient parameters are estimated as unknown parameters in the process. Global Mapping Function (GMF) is used to map the slant tropospheric delay to zenith
Displacement	Solid earth tides, solid earth pole tides, ocean tide loading correction (FES2004) and relativistic effects modelled by IERS Convention 2010
Reference time system	GPS Time
Receiver clock error	Single-difference between-satellite

The default elevation-dependant stochastic model for observations is represented by:

$$\sigma^2 = [c^2 + \frac{d^2}{(\sin e)^2}] \quad (13)$$

Equation (13) is similar to that implemented in RTKLIB (Takasu 2013), where  $e$  represents the satellite elevation,  $c$  and  $d$  are often set to 0.003m for a single carrier-phase measurement. The measurement noise for a single pseudorange measurement is empirically chosen around 100 or 150 times of that for phase measurements. The data were processed in PPP with float and fixed carrier phase ambiguities.

#### 4. DUAL- AND TRIPLE-FREQUENCY PPP RESULTS

The performance of dual-frequency PPP and triple-frequency PPP can be assessed by the integer ambiguity resolution success rate as well as the Root Mean Square (RMS) of horizontal and vertical position error. Note that the triple-frequency PPP results were based on a mix of dual- and triple-frequency GPS observables. The RMS is computed based on the differences between the known coordinates of the ARGN stations as shown in Table 1 with the position estimates provided from PPP.

Figure 5 and Figure 6 show the horizontal and vertical RMS of the dual- and triple-frequency float and ambiguity-fixed PPP, respectively. The solid line in these figures represents the triple-frequency solution, and the dash line presents the dual-frequency solution.

As it can be seen from Figure 5, the float solution requires at least 22 minutes to converge within 0.1m horizontally and vertically of the known position. On the other hand, triple-frequency PPP provides a slight improvement of 1 to 3cm when compared to dual-frequency PPP. After 25 minutes, both dual- and triple-frequency solutions are comparable and the solutions converge to about 8cm after 1.5 hours.

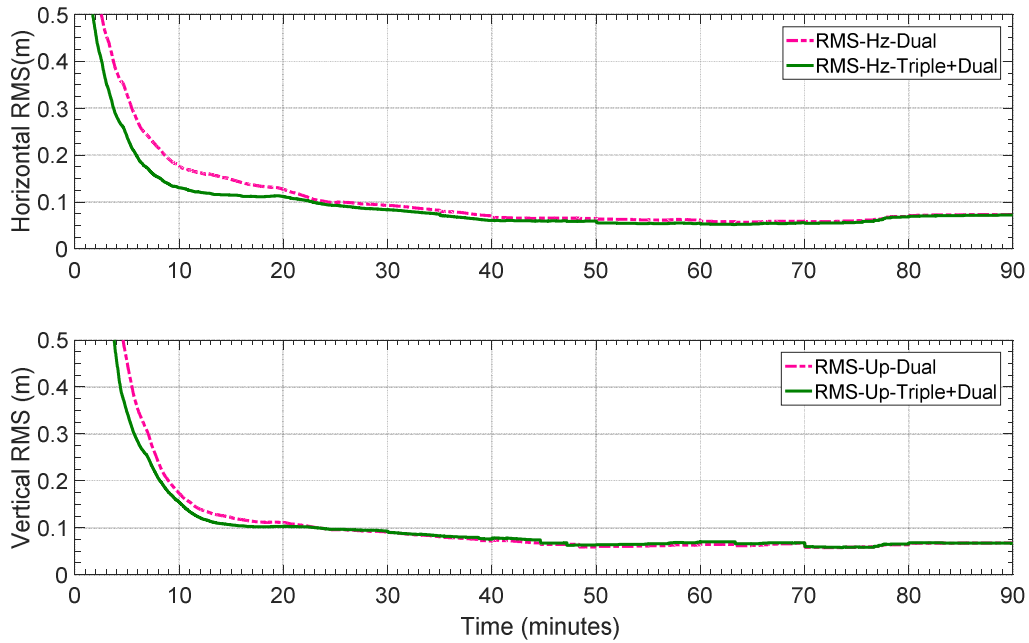


**Figure 5.** PPP convergence comparison between dual- and triple-frequency scenarios (float solution) with combined RMS from eight selected stations

In contrast to Figure 5 (float-PPP), NL ambiguity resolution is able to shorten the PPP solution convergence time as shown in Figure 6 (fixed-PPP). This is because in the fixed solution, the NL ambiguity can be resolved correctly thus providing the highest positioning accuracy. In order to achieve 10cm RMS for both horizontal components, triple- and dual-frequency with fixed ambiguity method require 9 to 14 minutes, respectively. Similarly, the amount of time for triple- and dual-frequency to reach 10cm of accuracy level in vertical component is 10 to 12 minutes, respectively. After that, both dual- and triple-frequency PPP scenarios remain unchanged at 4cm RMS level after 30 minutes of observations.

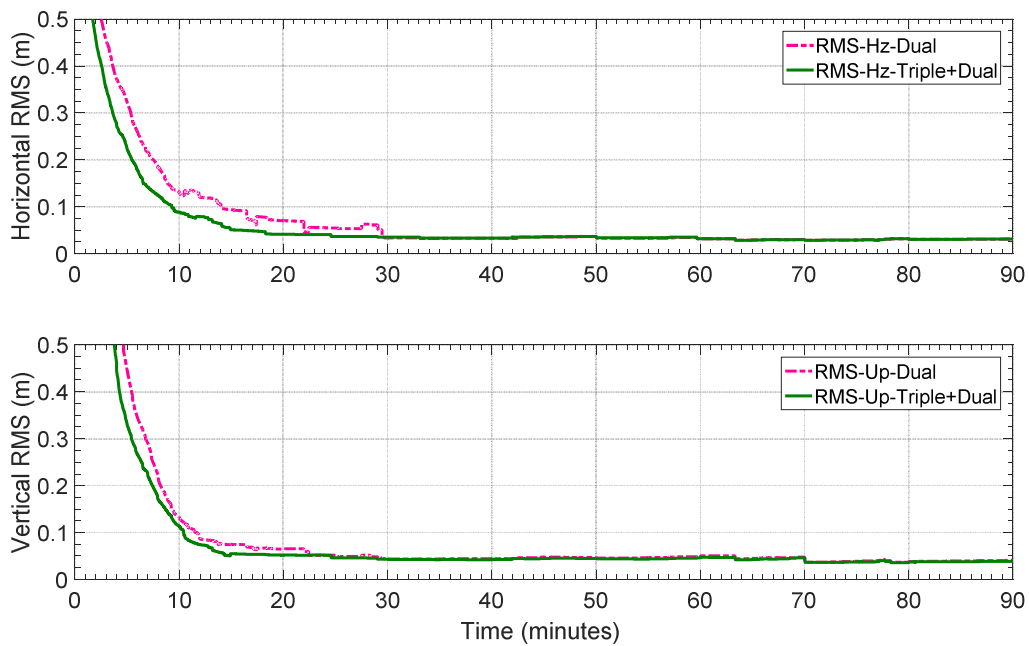


**Figure 6.** PPP convergence comparison between dual- and triple-frequency scenarios (fixed solution)

with combined RMS from eight selected stations

The ambiguity fixing rates for dual- and triple-frequency PPP are shown in Figure 7. The ambiguity-fixing rate of triple-frequency PPP scenario is about 10% higher than dual-frequency PPP for the first 15 minutes of observations. Both dual- and triple-frequency solutions show an exponential trend with dual- and triple-frequency PPP achieving more than 95% ambiguity fixing rate after 20 minutes.

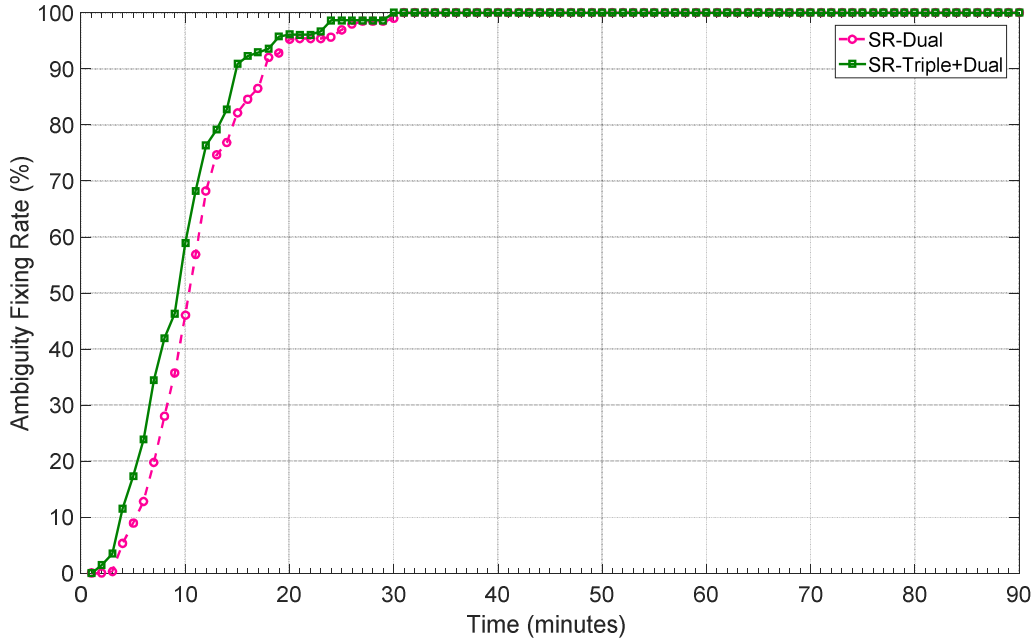


**Figure 7.** PPP convergence comparison for ambiguity fixing rates between dual- and triple-frequency (with combined results from eight selected stations)

Table 3 is a summary of the convergence times required for dual- and triple-frequency PPP solutions with float and fixed ambiguities within < 5cm, < 10cm and < 15cm of the known values for both horizontal and vertical components. The average convergence time required by the PPP solutions to reach the specified accuracy levels (i.e. <5cm, 10cm and 15cm) using triple-frequency is about 5 minutes less than that using dual-frequency observations. In addition, the average time required by the PPP-fixed ambiguity solution to achieve 5cm positioning accuracy is approximately 20 minutes. However, for the float ambiguity PPP solutions, this level of positioning cannot be achievable after 1.5 hours.

**Table 3.** Positioning convergence time with combined results from eight selected stations

Horizontal RMS threshold	Convergence time (minutes)				Vertical RMS threshold	Convergence time (minutes)			
	Dual float	Dual fixed	Triple float	Triple fixed		Dual float	Dual fixed	Triple float	Triple fixed
< 5cm	N/A	22	N/A	17	< 5cm	N/A	26	N/A	17
< 10cm	25	15	23	10	< 10cm	24	12	24	10

< 15cm	15	9	9	7	< 15cm	12	10	11	7
--------	----	---	---	---	--------	----	----	----	---

\*N/A: Data collected is not enough to reach accuracy levels.

## 5. CONCLUDING REMARKS

The modernised GPS Block IIF satellites offer an additional signal frequency and observable, which can strengthen the positioning model of PPP and thereby improving the positioning accuracy and solution convergence time. This paper describes the performance of dual-frequency and triple-frequency PPP in static mode. The benefits of triple-frequency PPP system were evaluated and compared using real observations collected from eight CORS in Australia. It was shown that triple-frequency measurements could help to improve the float ambiguity positioning accuracy and shorten the convergence time by an average of 5 minutes when compared to dual-frequency PPP. The ambiguity fixing success rate is also increased by 10% when using triple-frequency measurements, thereby improving the estimated positioning accuracy. It is envisaged that the solution convergence time can be further reduced with increased number of GNSS satellites, such as when the GPS Block III satellites are launched. Future research will include investigation into the benefits of adding multi-constellation and multi-frequency GNSS to the PPP model. In addition, the use of multi-frequency and multi-constellation GNSS will be expanded in kinematic mode.

## ACKNOWLEDGEMENTS

Geoscience Australia is gratefully acknowledged for providing the GPS data from the Australian Regional GNSS Network. Australia Award Scholarships (AAS) is also gratefully acknowledged for supporting the first author to pursue his PhD at RMIT University, Melbourne, Australia.

## REFERENCES

- Choy, S., Bisnath, S. & Rizos, C. 2016, Uncovering common misconceptions in GNSS Precise Point Positioning and its future prospect, *GPS Solutions*.
- CNES 2016, *The PPP-WIZARD project*, 2016, <<http://www.ppp-wizard.net/ssr.html>>.
- Collins, P. 2008, Isolating and Estimating Undifferenced GPS Integer Ambiguities.
- Collins, P. & Bisnath, S. 2011, Issues in Ambiguity Resolution for Precise Point Positioning.
- El-Mowafy, A., Deo, M. & Rizos, C. 2016, On biases in precise point positioning with multi-constellation and multi-frequency GNSS data, *Measurement Science and Technology*, vol. 27, no. 3, p. 035102.
- Ge, M., Gendt, G., Rothacher, M., Shi, C. & Liu, J. 2008, Resolution of GPS carrier-phase ambiguities in Precise Point Positioning (PPP) with daily observations, *Journal of Geodesy*, vol. 82, no. 7, pp. 389-99.
- Geng, J. H. 2010, Rapid Integer Ambiguity Resolution in GPS Precise Point Positioning, the University of Nottingham.
- Geng, J. H. & Bock, Y. 2013, Triple-frequency GPS precise point positioning with rapid ambiguity resolution, *Journal of Geodesy*, vol. 87, no. 5, pp. 449-60.
- Geng, J. H., Meng, X. L., Dodson, A. H., Ge, M. R. & Teferle, F. N. 2010a, Rapid re-convergences to ambiguity-fixed solutions in precise point positioning, *Journal of Geodesy*, vol. 84, no. 12, pp. 705-14.
- Geng, J. H., Meng, X. L., Dodson, A. H. & Teferle, F. N. 2010b, Integer ambiguity resolution in precise point positioning: method comparison, *Journal of Geodesy*, vol. 84, no. 9, pp. 569-81.
- Geoscience-Australia 2016, 2016, <<ftp://ftp.ga.gov.au/geodesy-outgoing/gnss/solutions/final/weekly/>>.
- Hofmann, W. B., Lichtenegger, H. & Wasle, E. 2008, *GNSS – Global Navigation Satellite Systems: GPS, GLONASS, Galileo, and more*, Springer WienNewYork.
- IGS 2016, *International GNSS Service*, 2016, <<http://www.igs.org/>>.
- Kouba, J. 2009, A Guide To Using International GNSS Service (IGS) Products, Geodetic Survey Division,

Natural Resources, Canada.

- Laurichesse, D. 2012, Phase Biases Estimation for Undifferenced Ambiguity Resolution, paper presented to PPP-RTK & Open Standards Symposium, Frankfurt, Germany.
- Laurichesse, D. 2015, Handling the Biases for Improved Triple-Frequency PPP Convergence, *GPSWorld*.
- Laurichesse, D. 2016, Fast PPP Convergence Using Multi-Constellations And Triple-Frequency Ambiguity Resolution, paper presented to IGS, Australia.
- Laurichesse, D., Flavien, M., Jean-Paul, B., Patrick, B. & Luca, C. 2009, Integer Ambiguity Resolution on Undifferenced GPS Phase Measurements and Its Application To PPP And Satellite Preciseorbit Determination, *Journal of The Institute of Navigation*, vol. 56, no. 2.
- Laurichesse, D., Mercier, F. & Berthias, J. P. 2010, Real-time PPP with Undifferenced Integer Ambiguity Resolution, Experimental Results.
- Laurichesse, D., Mercier, F., Berthias, J. P. & Bijac, J. 2008, Real time zero difference ambiguities blocking and absolute RTK, *ION NTM-2008*, San Diego, California.
- Li, T., Wang, J. & Laurichesse, D. 2013, Modeling and quality control for reliable precise point positioning integer ambiguity resolution with GNSS modernization, *GPS Solutions*, vol. 18, no. 3, pp. 429-42.
- Rizos, C., Janssen, V., Roberts, C. & Grinter, T. 2012, Precise Point Positioning: Is the Era of Differential GNSS Positioning Drawing to an End?, *FIG Working Week*, Rome, Italy.
- Security, U. S. D. o. H. 2016, viewed 31 August 2016, <<http://navcen.uscg.gov/?Do=constellationStatus>>.
- Shi, J. 2012, Precise Point Positioning Integer Ambiguity Resolution with Decoupled Clocks, University of Calgary.
- Shi, J. & Gao, Y. 2013, A comparison of three PPP integer ambiguity resolution methods, *GPS Solutions*, vol. 18, no. 4, pp. 519-28.
- Takasu, T. 2013, RTKLIB ver. 2.4.2 Manual.
- Takasu, T. 2016, RTKLIB: An Open Source Program Package for GNSS Positioning.
- Teunissen, P. J. G. 1993, Least-Squares Estimation of the Integer GPS Ambiguities, August 1993.
- Teunissen, P. J. G. & Khodabandeh, A. 2014, Review and principles of PPP-RTK methods, *Journal of Geodesy*, vol. 89, no. 3, pp. 217-40.
- Verhagen, S. & Teunissen, P. J. G. 2013, The ratio test for future GNSS ambiguity resolution, *GPS Solutions*, vol. 17, no. 4, pp. 535-48.
- Zhao, Q., Sun, B., Dai, Z., Hu, Z., Shi, C. & Liu, J. 2015, Real-time detection and repair of cycle slips in triple-frequency GNSS measurements, *GPS Solutions*, vol. 19, no. 3, pp. 381-91.
- Zumberge, J. F., Heflin, M. B., Jefferson, D. C., Watkins, M. M. & Webb, F. H. 1997, Precise point positioning for the efficient and robust analysis of GPS data from large networks, *Journal of Geophysical Research: Solid Earth*, vol. 102, no. B3, pp. 5005-17.